



# Compressibility studies of RE<sub>6</sub>UO<sub>12</sub> at extreme conditions of pressure

BALMUKUND SHUKLA<sup>1,\*</sup>, N R SANJAY KUMAR<sup>1</sup>, HRUDANANDA JENA<sup>2</sup>, ANUJ UPADHYAY<sup>3</sup> and N V CHANDRA SHEKAR<sup>1</sup>

<sup>1</sup>High Pressure Physics Section, Condensed Matter Physics Division, Indira Gandhi Centre for Atomic Research, Kalpakkam 603102, India

<sup>2</sup>Materials Chemistry Division-Chemistry Group, Indira Gandhi Centre for Atomic Research, Kalpakkam 603102, India

<sup>3</sup>Synchrotron Utilization Section, Raja Ramanna Center for Advanced Technology, Indore 452013, India

\*Author for correspondence (bshukla@igcar.gov.in)

MS received 10 May 2022; accepted 20 June 2022

**Abstract.** Rare-earth uranates-RE<sub>6</sub>UO<sub>12</sub> are synthesized by heating mixture of uranium oxide and rare-earth oxides in 1:6 ratio above 1273 K. These compounds stabilize in rhombohedral structure at ambient. High-pressure (HP) X-ray diffraction studies reveal that the compounds are stable at lower pressures, beyond which disorder is seen to originate and compound has a tendency to amorphize at very HPs. The *a*-axis of the lattice is found to be more rigid as compared to *c*-axis because of corner sharing polyhedra along *a*-axis. Anomalous compressibility behaviour is seen in Gd<sub>6</sub>UO<sub>12</sub>, where sharp decrease in the bulk modulus is observed. The behaviour is against the normal trend of compressibility in RE<sub>6</sub>UO<sub>12</sub> compounds along rare-earth cation series.

**Keywords.** High pressure; compressibility; order–disorder transition; actinides.

## 1. Introduction

The behaviour of materials under extreme conditions has been under intense study for decades. Actinides, being reactor fuel materials, are among the most studied materials from technological and physics point of view; hence, the study of its compounds are desirable under extreme conditions. Uranate compounds are ternary oxides, where the element uranium is in any one of the following oxidation states of +4, +5 or +6. The typical chemical formula of uranate is RE<sub>x</sub>U<sub>y</sub>O<sub>z</sub>, where RE represents a cation. RE-U-O phase diagram has been reported long back in the literature [1]. In the phase diagram, RE<sub>6</sub>UO<sub>12</sub> (RE = rare-earth elements) type of compounds, called rare-earth uranates, form by heating a mixture of uranium oxide and rare-earth oxides (in a ratio of 1:6, respectively) above 1273 K. Rare-earth uranates-RE<sub>6</sub>UO<sub>12</sub> exist in the rhombohedral structure at ambient [2–4].

High-temperature X-ray diffraction (XRD) studies show positive thermal expansion coefficient for all RE<sub>6</sub>UO<sub>12</sub> (RE—La, Gd, Nd, Sm, Eu, Tb and Dy). A general trend of decrease in the thermal expansion coefficient as a function of atomic number of the cation (RE<sup>3+</sup>) is seen, again it is due to the smaller unit cell size of the lattice

from La to Dy uranate. The thermal expansion coefficient of the compound is found to be maximum, whereas its heat capacity is minimum in the RE cation series of RE<sub>6</sub>UO<sub>12</sub> compounds. Other rare-earth oxide compounds, such as RE<sub>2</sub>O<sub>3</sub> (rare-earth sesquioxides) [5] and RE<sub>2</sub>Zr<sub>2</sub>O<sub>7</sub> (rare-earth zirconates) [6], too, show similar behaviour in their physical properties, e.g., thermal expansion coefficient and heat capacity. In rare-earth sesquioxides, the anomalous behaviour is ascribed to the half-filled 4*f* states [7]. Rare-earth uranates also show the same behaviour. Thermal expansion coefficient is always more along *a*-axis than *c*-axis, except, in Gd<sub>6</sub>UO<sub>12</sub> [8,9]. Jena *et al* [10] accredits the effect to the rigidity of the crystal along *c*-axis. Sahu *et al* [9] reported a much higher thermal expansion coefficient along *c*-axis ( $\alpha_c$ ) in Gd<sub>6</sub>UO<sub>12</sub> and attributed it to increased coulombic repulsion between two adjacent cations (Gd<sup>3+</sup>) due to small cationic radii [9]. The same effect of increased coulombic repulsion does not appear in Dy<sub>6</sub>UO<sub>12</sub>, where  $\alpha_a$  is again found to be more than  $\alpha_c$  and it remains an open question to be explained. The lattice thermal expansion coefficients increase with increasing temperature and expansion is more along the *a*-axis compared to the *c*-axis [8–12]. It is attributed to lesser density of atoms along the *a*-axis.

As these rare-earth uranates show very interesting changes in their thermophysical properties, their high-

This article is part of the Special issue on ‘High pressure materials science: recent trends’.

pressure (HP) properties are expected to bring forward hitherto unknown changes. Here, we report *in-situ* HP structural stability studies on rare-earth uranates (RE = Sm, Gd, Dy).

## 2. Experimental

### 2.1 Sample preparation and characterization

The sample was prepared using the urea-combustion method [13,14]. X-ray diffraction (XRD) pattern was taken at ambient conditions using synchrotron X-ray source to affirm the phase formation. All the peaks in the diffraction pattern could be indexed to the rhombohedral structure with space group R-3, which confirms the formation of the compound in a single phase with rhombohedral structure. The lattice parameters were obtained by least square fitting of  $2\theta$  reflections using NIST\*AIDS-83 software. The lattice parameters of various  $\text{RE}_6\text{UO}_{12}$  compounds, by analysis of the XRD, are shown in table 1 and they are in agreement with the values quoted in the literature [10].

### 2.2 Techniques used for high-pressure experiment at ambient temperature

High-pressure X-ray diffraction (HP-XRD) experiments on the polycrystalline sample of  $\text{RE}_6\text{UO}_{12}$  (RE = Sm, Gd, Dy) were carried out using a Mao-Bell type Diamond Anvil Cell (DAC). Synchrotron X-ray source at Beamline-12, INDUS-2, RRCAT, Indore, was used for HP-XRD studies on  $\text{RE}_6\text{UO}_{12}$ . Silver was used as the pressure calibrant, as its peaks do not overlap with sample peaks. A mixture of methanol:ethanol:water (MEW) in the ratio of 16:3:1 was used to obtain hydrostatic pressure environment inside the sample chamber of DAC. The compound was pressurized in steps to study the compressibility behaviour at ambient temperature. XRD patterns were collected for 10 min, at each pressure, in angle-dispersive mode and transmission geometry. mar345 IP detector was used for collecting diffracted X-rays and obtained 2D data were converted to  $2\theta$  vs. intensity using Fit2D software [15]. NIST\*AIDS-83 software was used to get the lattice parameters at various pressures. XRD study was carried out on compounds  $\text{RE}_6\text{UO}_{12}$  (RE = Sm, Gd, Dy) using synchrotron radiation

up to a pressure of 42, 70 and 28 GPa, respectively. The pressure was dropped slowly in steps and diffraction patterns were taken after a relaxation time of 30 min at each step in the reverse cycle.

## 3. Results and discussion

### 3.1 High-pressure study of $\text{RE}_6\text{UO}_{12}$ (RE = Sm, Gd, Dy) at ambient temperature

The materials  $\text{Sm}_6\text{UO}_{12}$ ,  $\text{Gd}_6\text{UO}_{12}$  and  $\text{Dy}_6\text{UO}_{12}$  have been studied under HP up to  $\sim 42$ ,  $\sim 70$  and  $\sim 28$  GPa,

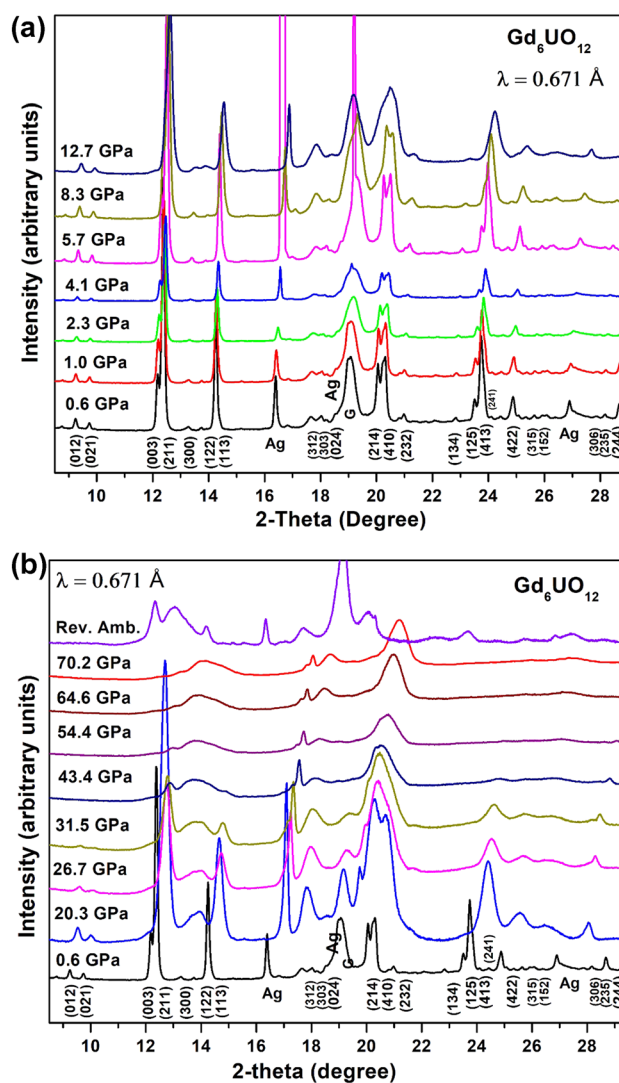


**Figure 1.** HP-XRD plots of  $\text{Gd}_6\text{UO}_{12}$  using synchrotron source at (a) lower pressure and (b) higher pressure showing disorder in the system. G and Ag represent reflections from SS gasket and silver, respectively. A sudden increase in the intensity of Ag at 5.7 GPa is due to preferred orientation of silver. Since, Bragg reflections of sample and pressure calibrant does not overlap, the preferred orientation in Ag has not affected the estimation of  $2\theta$  values of these reflections of sample as well as pressure calibrant.

**Table 1.** Lattice parameters of various  $\text{RE}_6\text{UO}_{12}$  compounds.

Compounds	Lattice parameters
$\text{Sm}_6\text{UO}_{12}$	$a = 10.153 \text{ \AA}$ , $c = 9.625 \text{ \AA}$
$\text{Gd}_6\text{UO}_{12}$	$a = 10.075 \text{ \AA}$ , $c = 9.534 \text{ \AA}$
$\text{Dy}_6\text{UO}_{12}$	$a = 9.9806 \text{ \AA}$ , $c = 9.4403 \text{ \AA}$

respectively. We have previously reported HP-XRD plots for  $\text{Sm}_6\text{UO}_{12}$  and  $\text{Dy}_6\text{UO}_{12}$  in the literature [16,17]. The angle-dispersive XRD patterns of  $\text{Gd}_6\text{UO}_{12}$  are shown in figure 1a and b at selected pressures. The evolution of the reflections in the diffraction patterns show that materials remain in the rhombohedral structure. It is evident from the diffraction patterns that all the Bragg peaks are well traceable up to 20.0 GPa. Moreover, the XRD reflections for  $\text{Sm}_6\text{UO}_{12}$  and  $\text{Dy}_6\text{UO}_{12}$  are reported to be traceable up to 28.0 and 21.6 GPa, respectively. The HP diffraction data are mapped to the rhombohedral structure and lattice parameters have been obtained using NIST\*AIDS-83 software. Lattice parameters  $a$  and  $c$  decrease in a linear fashion with increasing pressure, which is due to the isotropic compression of the unit cell of the lattice. The lattice-parameter variations of  $\text{Gd}_6\text{UO}_{12}$  with respect to pressure are shown in figure 2.

Apart from the usual contraction of lattice parameters under pressure, different rates of change in the ‘ $a$ ’ and ‘ $c$ ’ values of the rhombohedral structure are observed, i.e., the values of rate of change in lattice parameter with respect to pressure are different for each of the compounds, which are listed in table 2. It shows that  $\left(\frac{dc}{dP}\right)$  is always greater compared to  $\left(\frac{da}{dP}\right)$  implying that compression along  $c$ -axis is more compared to  $a$ -axis. Larger drop in the  $c$ -axis implies that  $c$ -axis compresses more readily and the ratio  $c/a$  decreases. This indicates that  $a$ -axis is more rigid under pressure as compared to  $c$ -axis. The rigidity of the  $a$ -axis with respect to pressure can be addressed using the polyhedral representation of the unit cell and Pauling rule for ionic structures. The crystal structure of  $\text{RE}_6\text{UO}_{12}$  can be visualized using polyhedra representation wherein, two  $\text{UO}_6$  polyhedra are separated by two  $\text{REO}_6$  polyhedra along the  $c$ -axis. A unit cell of the compound is shown in figure 3. Two  $\text{REO}_6$  polyhedra share edges, whereas  $\text{UO}_6$  and  $\text{REO}_6$  polyhedra are linked

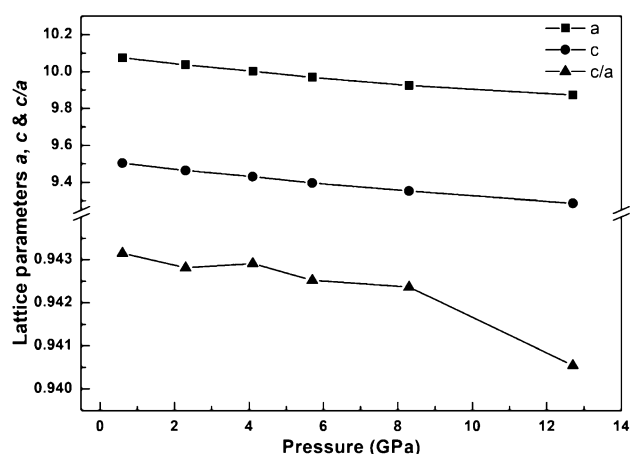


**Figure 2.** Variation of lattice parameter in  $\text{Gd}_6\text{UO}_{12}$  with respect to pressure.

**Table 2.** Rate of change in the lattice parameters with respect to pressure.

Compound	$\left(\frac{da}{dP}\right)$ at 293 K (Å GPa <sup>-1</sup> )	$\left(\frac{dc}{dP}\right)$ at 293 K (Å GPa <sup>-1</sup> )
$\text{Sm}_6\text{UO}_{12}$	0.0145	0.0174
$\text{Gd}_6\text{UO}_{12}$	0.0190	0.0223
$\text{Dy}_6\text{UO}_{12}$	0.0150	0.0180

at one corner. Corner-sharing is considered to be more stable as compared to the edge-sharing by Pauling’s rule for ionic structures. Hence, the compression along the edge-sharing  $\text{REO}_6$  polyhedra is more at HPs. The converse happens along the  $c$ -axis where  $\text{REO}_6$  and  $\text{UO}_6$  share edges. Moreover, there are more number of polyhedra along  $a$ -axis as compared along  $c$ -axis. Since polyhedra determine bonding nature of the crystal and number of bonds are more along  $a$ -axis, therefore, making it difficult to compress. Thus, the Pauling’s rule for ionic structure and more number of polyhedra along  $a$ -axis, justify the observed trend in the lattice parameter variation as a function of pressure.

It is noticeable that rhombohedral reflections are traceable up to the pressure 28.0, 20.0 and 21.6 GPa for the compounds  $\text{Sm}_6\text{UO}_{12}$ ,  $\text{Gd}_6\text{UO}_{12}$  and  $\text{Dy}_6\text{UO}_{12}$ , respectively. The pressure–volume data have been fitted to 3rd order Birch Murnaghan Equation of State (BM-EOS) (figure 4) [18]. The nonlinear BM-EOS fit yields bulk modulus 157.7, 134.1 and 144.0 GPa for  $\text{Sm}_6\text{UO}_{12}$ ,  $\text{Gd}_6\text{UO}_{12}$  and  $\text{Dy}_6\text{UO}_{12}$ , respectively. The bulk modulus vs. atomic number of cation ( $\text{RE}^{3+}$ ) is plotted in figure 5. The bulk modulus is expected to decrease continuously as the atomic number of the cation increases. The reason is the decrease in cation- $\text{RE}^{3+}$  radius, which results in a decrease in cation–cation distance. Shorter cation–cation distance increases the repulsion between them, causing instability of the lattice. Moreover, lesser cationic radius causes localization of the 4- $f$  electron and hence weaker bonding.  $\text{Sm}_6\text{UO}_{12}$  and  $\text{Dy}_6\text{UO}_{12}$  follow the usual trend

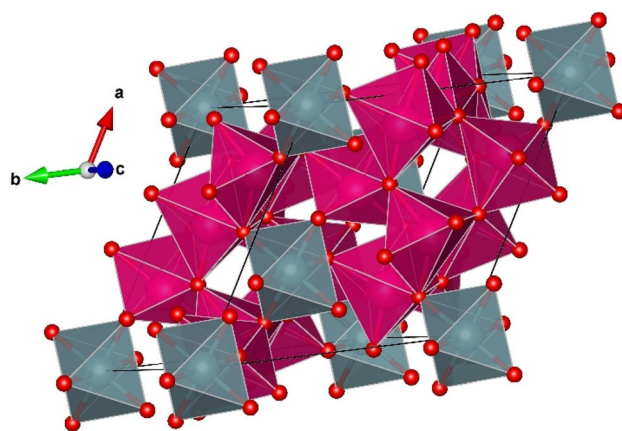


**Figure 3.** Polyhedral representation of unit cell of  $\text{RE}_6\text{UO}_{12}$ .

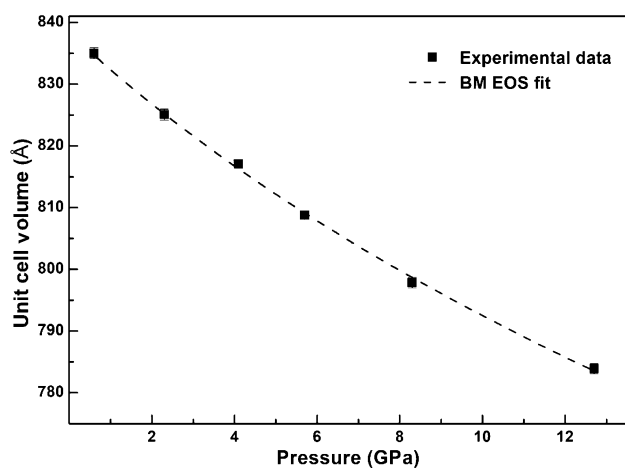


**Figure 4.** Estimated unit cell volume of  $Gd_6UO_{12}$  at various pressures and its BM-EOS fitting.

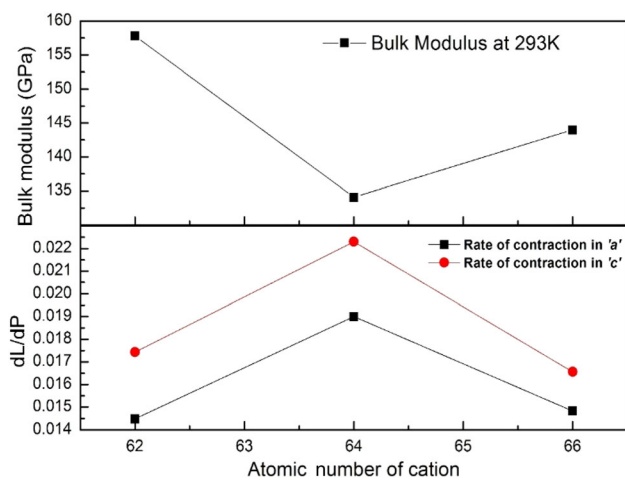


**Figure 5.** Bulk modulus (top) and rate of change of lattice parameters (bottom) with pressure ( $dL/dP$ ) as a function of atomic number of cation.

of decrease in the bulk modulus. However, a sudden drop in the bulk modulus has been observed in  $Gd_6UO_{12}$  (figure 5, top), indicating  $Gd_6UO_{12}$  to be a softer compound. The same is reflected in the lattice parameters (figure 5, bottom) where it follows the similar trend. The rate of decrease in lattice parameters of  $Gd_6UO_{12}$  is found to be higher compared to that of  $Sm_6UO_{12}$  and  $Dy_6UO_{12}$  (figure 5, bottom). The abnormality in the bulk modulus of the compound may be explained in terms of localization of electrons. Gadolinium has half-filled 4-*f* orbitals, which is considered to be stable compared to the partially filled orbitals, indicating that these outer shell 4-*f* electrons are localized and do not participate in the bonding. The density of states and charge density calculations are required to quantitatively explain the nature of bonding, its variations with respect to pressure and the localization of the 4-*f* electrons in  $Gd_6UO_{12}$ , which has been seen in our HP experiments.

Beyond a certain pressure, large peak broadening indicates setting of disorder in the compound. Similar disorder has already been seen in  $Sm_6UO_{12}$  and  $Dy_6UO_{12}$  and explained in terms of anion disorder followed by cation disorder at higher pressures [16,17]. When the pressure is further applied on these compound, i.e. beyond 28.0, 20.0 and 21.6 GPa in  $Sm_6UO_{12}$ ,  $Gd_6UO_{12}$  and  $Dy_6UO_{12}$ , respectively, the peaks broaden in such a manner that peaks are not traceable and the quality of data is not amenable for refinement or lattice parameter estimation. The disorder in the system sets in, which further increases at higher pressures. The disorder is found to increase such that the system has a tendency to amorphize at HPs. The onset of disorder in compounds  $Sm_6UO_{12}$ ,  $Gd_6UO_{12}$  and  $Dy_6UO_{12}$  appears at different pressures like  $\sim 27$ ,  $\sim 20$  and  $\sim 21$  GPa, respectively. The trend in the bulk modulus and the disorder pressure are found to be similar. Therefore, the conclusion can be arrived in the terms of compressibility, which affirms that softer compounds get easily distorted and amorphized at lower pressures than those having lower compressibility.

#### 4. Conclusion

High-pressure studies on  $Sm_6UO_{12}$ ,  $Gd_6UO_{12}$  and  $Dy_6UO_{12}$  have been carried out using synchrotron source at ambient temperature. The study reveals that the compounds are stable at lower pressures. The *a*-axis of the lattice is found to be more rigid as compared to *c*-axis because of its corner-sharing polyhedra along *a*-axis. The bulk moduli of the compounds  $Sm_6UO_{12}$ ,  $Gd_6UO_{12}$  and  $Dy_6UO_{12}$  are estimated to be 157.7, 134.1 and 144.0 GPa, respectively. An abrupt softening in  $Gd_6UO_{12}$  has been observed, which can be ascribed to the localization of 4-*f* electrons of Gd. At lower pressure, disorder in the system originates. The disorder was ascribed to anion disorder followed by cation disorder. Beyond  $\sim 20$  GPa, the disorder increased to such an extent that the compound has a tendency to amorphize when both the anion and cation disorder takes place simultaneously. The disorder pressure in the system has a correlation with the compressibility of the compound, where disorder at lower pressures was seen in the compound with high compressibility.

#### Acknowledgements

We thank the members of High Pressure Studies Section at IGCAR. We also thank IGCAR management for their support.

#### References

- [1] Berndt U, Tanamas R and Keller C 1976 *J. Solid State Chem.* **17** 113

- [2] Hinatsu Y, Masaki N and Fujino T 1988 *J. Solid State Chem.* **73** 567
- [3] Diehl H G and Keller C 1971 *J. Solid State Chem.* **3** 621
- [4] Aitken E A, Bartram S F and Juenke E F 1964 *Inorg. Chem.* **3** 949
- [5] Taylor D 1984 *Trans. J. Br. Ceram. Soc.* **83** 92
- [6] Lehmann H, Pitzer D, Pracht G, Vassen R and Stöver D 2003 *J. Am. Ceram. Soc.* **86** 1338
- [7] Zinkevich M 2007 *Prog. Mater. Sci.* **52** 597
- [8] Venkata Krishnan R, Babu R, Panneerselvam G, Ananthasivan K, Antony M P and Nagarajan K 2012 *Ceram. Int.* **38** 5277
- [9] Sahu M, Krishnan K, Saxena M K and Ramakumar K L 2009 *J. Alloys Compd.* **482** 141
- [10] Jena H, Asuvathraman R and Kutty K V G 2000 *J. Nucl. Mater.* **280** 312
- [11] Venkata Krishnan R, Jena H, Govindan Kutty K V and Nagarajan K 2010 *J. Therm. Anal. Calorim.* **101** 371
- [12] Sahu M, Krishnan K, Saxena M K and Dash S 2013 *J. Therm. Anal. Calorim.* **112** 165
- [13] Moore J J and Feng H J 1995 *Prog. Mater. Sci.* **39** 243
- [14] Moore J J and Feng H J 1995 *Prog. Mater. Sci.* **39** 275
- [15] Hammersley A P, Svensson S O, Hanfland M, Fitch A N and Häusermann D 1996 *High Press. Res.* **14** 235
- [16] Shukla B, Sanjay Kumar N R, Chandra Shekar N V, Jena H and Sinha A K 2019 *J. Alloys Compd.* **771** 1029
- [17] Shukla B, Sanjay Kumar N R, Sekar M, Chandra Shekar N V, Jena H and Asuvathraman R 2016 *J. Alloys Compd.* **672** 393
- [18] Birch F 1947 *Phys. Rev.* **71** 809